Edge flow measurements with Gundestrup probes*

J. P. Gunn†
Association Euratom—CEA sur la Fusion Contrôlée, DRFC Bâtiment 508, CEA Cadarache, 13108 Saint Paul Lez Durance, France

C. Boucher
INRS-Energie et matériaux, 1650 Lionel-Boulet, Varennes, Québec J3X 1S2, Canada

P. Devynck
Association Euratom—CEA sur la Fusion Contrôlée, DRFC Bâtiment 508, CEA Cadarache, 13108 Saint Paul Lez Durance, France

I. Ďuran
Institute of Plasma Physics, Association EURATOM/IPP.CR, Za Slovankou 3, P.O.B. 17, Praha 8, Czech Republic

K. Dyabilin
Institute for High Energy Densities, Moscow, Russia

J. Horaček, M. Hron, and J. Stöckel
Institute of Plasma Physics, Association EURATOM/IPP.CR. Za Slovankou 3, P.O.B. 17, Praha 8, Czech Republic

G. Van Oost and H. Van Goubergen
Department of Applied Physics, Ghent University, Rozier 44, 9000 Gent, Belgium

F. Žáček
Institute of Plasma Physics, Association EURATOM/IPP.CR, Za Slovenkou 3, P.O.B. 17, Praha 8, Czech Republic

(Received 23 October 2000; accepted 30 October 2000)

The ion current collected by a probe in a magnetized plasma is sensitive to the angle between its surface and the flow streamlines. This intuitive concept is the basis of the Gundestrup probe, a polar array of planar collectors mounted around an insulating housing. Probe theory for measuring flows has been developed on two fronts: Recent kinetic and fluid models, reviewed here, give similar predictions for the collected current within the range of applicability of the model assumptions. A comparison with measurements by a rotating Mach probe in the CASTOR tokamak (Czech Academy of Sciences Torus) [J. Stöckel, J. Badalec, I. Ďuran *et al.*, Plasma Phys. Controlled Fusion, **41**, 577 (1999)] highlights the role of magnetization in ion collection at grazing angles of incidence between the probe surface and the magnetic field lines. © *2001 American Institute of Physics.* [DOI: 10.1063/1.1344560]

I. INTRODUCTION

Main ion flow in the scrape-off layer is both the cause and the symptom of many tokamak edge phenomena. Plasma flow patterns are linked to the spatial distribution of recycling neutrals, and are expected to play a role in impurity control.[1] Convection competes with heat conduction in the power balance of recycling and detached discharges.[2] Tritium-rich carbon flakes that form preferentially on the inboard divertor louvres of JET (the Joint European Torus[3]) may be a result of poloidal flow in the scrape-off layer.[4] Ion–neutral flow differential gives rise to friction that can dominate over volume recombination in the detachment process.[5] Electric and ∇B drifts, along with their self-consistent radial and poloidal electric fields, are thought to be responsible for density asymmetries between the strike points.[6] Both the parallel and perpendicular components of the flow must be measured. It is insufficient, for example, to measure the parallel flow alone to conclude the existence of flow reversal out of the divertor. $E \times B$ drifts can easily counteract parallel flow due to the low pitch angle of the magnetic field lines, so parallel flow reversal may not necessarily imply total poloidal flow reversal.[7]

Probes are used to measure flow in many fusion research machines. Convincing consistency between measured changes of radial electric field and poloidal flows have been made in many tokamaks.[8–16] A simple technique is to use a Gundestrup probe[17] that consists of multiple conducting pins mounted around an insulating cylindrical housing [Fig. 1(a)] in order to measure the polar diagram of ion saturation current. Another approach was recently adopted[15] in the CASTOR tokamak (Czech Academy of Sciences Torus[18]) using a rotating Mach probe consisting of two back-to-back, flat plates, separated by an insulator [Fig. 1(b)]. Continuous ion current distributions allow a detailed comparison with

*Paper JI1 3, Bull. Am. Phys. Soc. **45**, 185 (2000).
†Invited speaker.

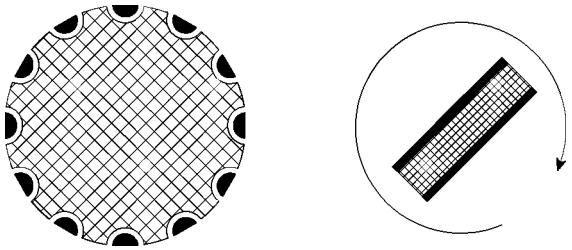

FIG. 1. On the left is a schematic of a 12-pin Gundestrup probe and on the right, a 2-plate rotatable Mach probe.

the models, and should help to evaluate whether there is some physics still missing from them. The basic philosophy of flow measurement with probes is to insert a solid body into the plasma and generate a local perturbation of the background flow field. Modeling provides the link between the measured ion current distribution and the unperturbed ion flow speed. If flow is present then one intuitively expects to measure larger ion current on the side of the probe that faces upstream than on the side that faces downstream into the probe wake. After brief reviews of a kinetic model[19] (Sec. II) and a fluid model[20] (Sec. III), the theoretical predictions will be compared with the CASTOR data in Sec. IV. The sensitivity of the fitted Mach numbers to angular misalignment of the probe will be analyzed in Sec. V.

II. KINETIC MODEL

A two-dimensional (2D) kinetic code called ''GUNDY'' has been developed to solve the ion motion in the wake of a cylindrical probe, and to calculate the ion current distribution over the surface. A description of and first results from this code can be found in Ref. 19. A quasineutral particle-in-cell (PIC) approach has been adopted. The parallel ion speed distribution in the absence of the probe is a shifted Maxwellian. A constant perpendicular drift is imposed on all ions. Only the guiding center motion is resolved. Diffusion is represented by a random walk in the perpendicular direction. The parallel electric field is calculated from the local ion density gradient assuming quasineutrality. All ions that impinge upon the probe are neutralized and disappear from the system.

An important test of the code is to run with a uniquely parallel drift velocity in order to compare with existing one-dimensional (1D) Mach probe models. In Fig. 2 the upstream-to-downstream current ratio is plotted against the parallel Mach number. The 2D PIC code agrees with the 1D fluid model of Hutchinson,[21] and the 1D kinetic model of Chung,[22] both of which include anomalous shear viscosity, but not with Stangeby's 1D fluid model[23] that does not. The reason is due to our choice of the diffusion mechanism: It is easy to show, following the arguments of Braginskii,[24] that the ratio of momentum diffusivity to particle diffusivity is exactly unity if the random walk step size is independent of the parallel speed, and if the parallel speed is unmodified by the diffusion process. Simultaneous measurements of parallel Mach number using laser-induced fluorescence (LIF) and a Mach probe[25] seem to favor the viscous models. The coherency of the results including uniquely parallel drift lend confidence to the following analysis of the effect of finite perpendicular drift.

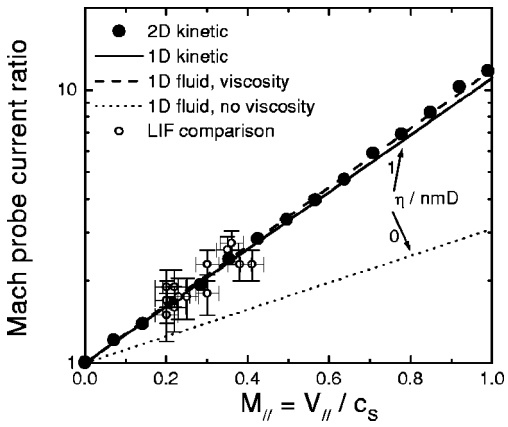

FIG. 2. Upstream-to-downstream ion saturation current ratio vs parallel Mach number. The full circles are the 2D kinetic results of Gunn. The solid line is the 1D kinetic model of Chung. The dashed line is the 1D fluid model of Hutchinson. The dotted line is the 1D fluid model of Stangeby. The open circles are the experimental LIF measurements of Poirier.

Figure 3 shows the PIC result for Mach numbers $M_{\parallel}=0.4$ and $M_{\perp}=0.3$. The flow streamlines are bent towards the probe in regions of strong density gradient near the edges of the wake. Parallel profiles of ion density, temperature, and parallel Mach number are shown in Fig. 4 for magnetic field lines passing just below, through the middle of, and just above the probe. The density is lower on the downstream side, as expected. The kinetic temperature in the presheath drops substantially towards the probe surface, contrary to the isothermal assumption adopted in fluid models. The curious heating on the top side of the probe is a kinetic effect caused by the intersection of two populations of fast ions with opposing velocities; those ions are accelerated in the upstream and downstream presheaths, but their trajectories narrowly miss the probe surface and continue upward. The parallel Mach number is invariably unity at the upstream and downstream faces having 90° magnetic field line incidence, independent of the perpendicular Mach number. We delay detailed analysis of the angular dependence of the ion current until after the description of the 1D fluid model in the next section.

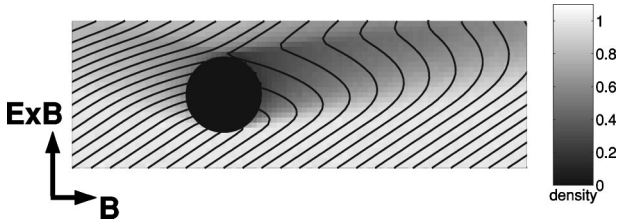

FIG. 3. Ion density distribution around a cylindrical probe in a magnetized plasma with flow Mach numbers $M_{\parallel}=0.4$ and $M_{\perp}=0.3$. The flow streamlines are superimposed.

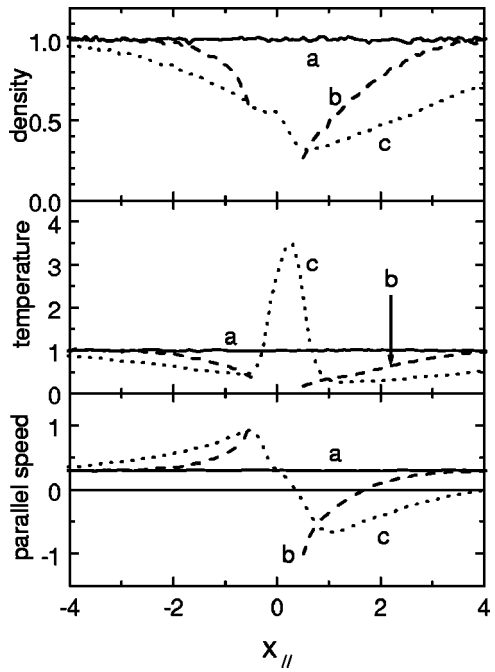

FIG. 4. Plasma parameters on field lines (a) just below, (b) through the middle of, and (c) just above the probe. The profiles of density (top panel), temperature (middle panel), and parallel Mach number (bottom panel) are shown.

III. FLUID MODEL

Van Goubergen[20] recently extended the 1D fluid model of Hutchinson[21] to include a finite perpendicular drift. The model equations are characterized by a singularity that determines the maximum parallel speed in the presheath; the singularity is assumed to occur at the magnetic presheath edge (MPSE):

$$M_{\parallel,\mathrm{MPSE}}=\frac{M_\perp}{\tan\,\alpha}+1.$$

This is the so-called ''intuitive'' or Bohm–Chodura boundary condition (B.–C. b.c.)[26] derived for the first time in a rigorous way from the transport equations. The B.–C. b.c. predicts that the parallel speed adapts itself in the presence of a perpendicular drift such that the normal projection of the total flow at the MPSE equals $c_S \sin\alpha$ where α is the angle between the surface and the magnetic field.

The important quantity for diagnostic applications is the MPSE ion flux. Since the fluid model is isothermal, the sheath edge density n_{MPSE} can also be used. Empirical fits to the numerical solution of the fluid model give

$$n_{\mathrm{MPSE}}=\exp[c_{\mathrm{up/down}}(\pm|M_{\parallel,\infty}|\mp|M_\perp|\cot\,\alpha)-1.05],$$

where the sign depends on whether the probe is looking upstream or downstream. The constant is well fitted by the expression

$$c_{\mathrm{up/down}}=1+0.14\,\exp(M_{\parallel,\infty}/0.862).$$

When the flow is null, $n_{\mathrm{MPSE}}=0.35$ in agreement with Hutchinson.[21]

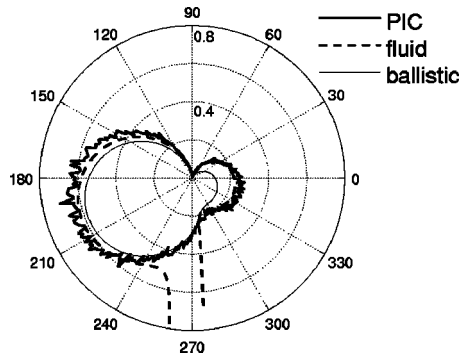

FIG. 5. Theoretical normally-directed ion current density onto an inclined surface as a function of angle. The thick curve is the GUNDY prediction, the dashed curve is the 1D fluid model of Van Goubergen, and the thin curve is the unidirectional thermal flux in the absence of electric fields. These are predictions for flow Mach numbers $M_\parallel=0.4$ and $M_\perp=0.3$.

The predicted angular distribution of ion current agrees very well with the GUNDY code except in the angular range where the model is known to break down (Fig. 5). The Van Goubergen model is limited to certain combinations of probe angle and flow speed. This is because the fluid boundary condition imposes sonic flow at the MPSE. If the normal projection of the perpendicular drift is large and towards the surface, then the B.–C. b.c. forces the parallel flow to diminish or even reverse. In the fluid model, the parallel speed at the MPSE must exceed the external Mach number because otherwise the density would increase unphysically towards the probe. The kinetic results show no evidence of singularities (Fig. 6). Rather, the bottom edge of the probe simply collects the incoming thermal ion flux, and the plasma near the surface is unperturbed. Notice that in the angular range where the fluid model breaks down, that the calculated kinetic ion flux is exactly equal to the ballistic thermal flux. This behavior can be explained with simple intuitive arguments as follows. Since all ions have the same perpendicular drift, we can consider the 2D spatial domain as a collection of 1D reference frames oriented parallel to the magnetic

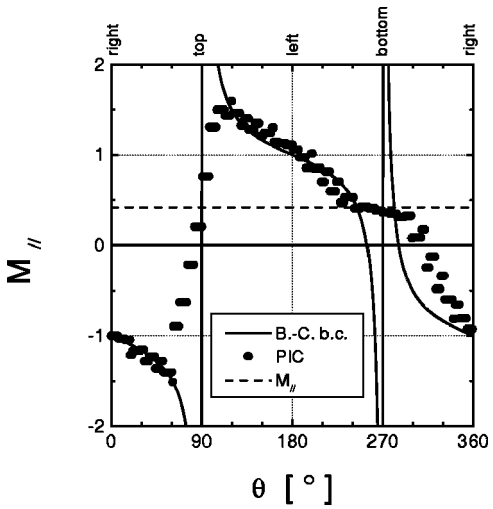

FIG. 6. Parallel Mach number at the MPSE around the probe. The full curve is imposed by the B.–C. b.c., and the points are from the GUNDY code. The dashed line shows the external parallel Mach number far from the probe.

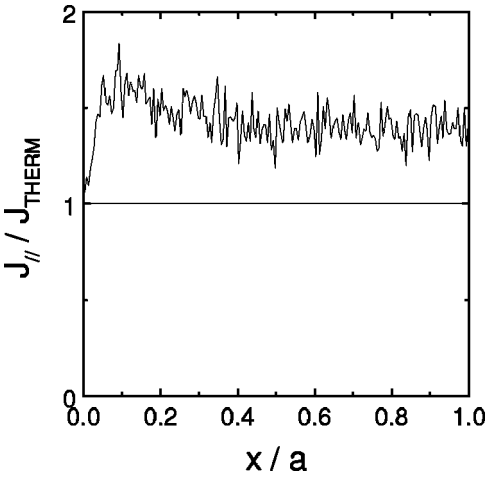

FIG. 7. Parallel current density onto a flat plate oriented at 90° with respect to the magnetic field. The plasma has flow Mach numbers $M_{\|}=0$ and $M_{\perp}=0.5$. The current is normalized by the Maxwellian thermal value.

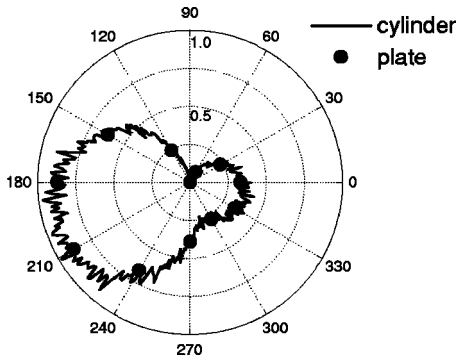

FIG. 8. Polar distribution of current calculated for a cylindrical probe (full curve) and a rotating Mach probe (points) for flow Mach numbers $M_{\|}=0.4$ and $M_{\perp}=0.3$.

field, drifting upwards towards the probe. The perpendicular coordinate is equivalent to time by the transformation $x_{\perp}=V_{\perp}t$. Assuming that the drift is large compared to any other cross field transport mechanism, the 1D plasma has no information about the existence of the probe until the first contact with the bottom edge. The sudden appearance of a particle sink in the local reference frame causes a density depression to propagate into the plasma at roughly the sound speed. It takes a short but finite time for the presheath potential drop to be established, and then, at a constant rate, the slowest receding ions are overtaken by the perturbation front, decelerated, reversed, and finally drawn back to the probe by the quasineutral electric field. The perturbation front corresponds to the leading edge of the wake in the 2D picture of Fig. 3. The expanding presheath has a self-similar structure; the current will remain constant as long as the probe is present in the system, or, equivalently, the plasma parameters are constant along the probe surface in 2D space. It is the constant, additional flux of reversed ions that increases the probe current above the thermal Maxwellian value. This conceptual picture is confirmed by PIC simulations of a flat Mach probe oriented at 90° to the magnetic field (Fig. 7). The ion flux onto the leading edge is almost exactly equal to the Maxwellian thermal flux, but it rapidly attains a larger value due to the action of the presheath potential drop. Further corroboration comes from measurements of the ion flux onto a biased divertor plate in Tokamak de Varennes which gave qualitative indications that the B.–C. b.c. could be oversatisfied in the presence of a strong radial electric field.[27]

IV. MEASUREMENTS IN THE CASTOR TOKAMAK

CASTOR is a tokamak with a circular plasma cross section. The principal parameters are major radius $R_{\mathrm{maj}}=40$ cm, minor radius $a_{\mathrm{min}}=8.5$ cm, toroidal magnetic field $B_T=1.0$ T, plasma current $I_P=25$ kA, and lower hybrid heating power 50 kW. A movable biasing electrode is used to tailor the edge radial electric fields, modify turbulence, and control edge flows.[28] In this section we will compare experimental polar diagrams of ion saturation current obtained from a recently installed rotatable Mach probe with the theoretical predictions.

The GUNDY code has been adapted to simulate the CASTOR probe geometry. Rather than a cylindrical probe (a circular boundary in the 2D plane), two flat collectors separated by an insulator have been simulated. The disadvantage of this model is that the code must be run for several angles in order to construct the polar diagram of ion current. In Fig. 8 we compare the ion current density collected by a cylindrical probe with that collected by the flat probe for parallel Mach number $M_{\|}=0.4$ and perpendicular Mach number $M_{\perp}=0.3$. It turns out that the flat plates collect exactly the same current density as a small surface element of a cylindrical probe for equal magnetic field angles, meaning that the cylindrical simulation results can be directly applied to the CASTOR probe geometry. In Fig. 8 one notices the usual disappearance of ion flux on top of the probe due to the fact that simulation ions only have upward-going trajectories. Real experimental data contradicts this prediction. In Fig. 9 is shown the ion current ratio measured by the parallel plates of the CASTOR rotatable Mach probe. The Van Goubergen model gives a good fit to within $\pm 30°$ of grazing magnetic field incidence. The corresponding GUNDY polar diagram is compared with the data in Fig. 10. There seems to be excess current on both the top and bottom of the probe that cannot

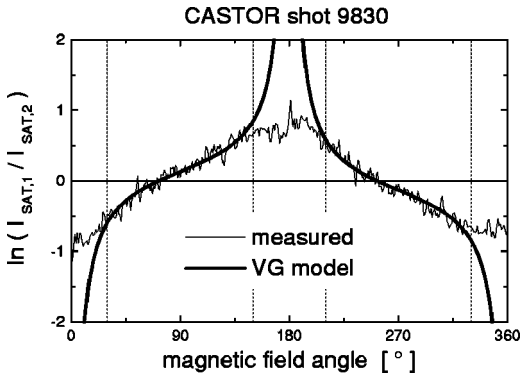

FIG. 9. The best fit of the Van Goubergen model to the measured current ratio in CASTOR. Points within 30° of tangency were excluded. The best fit gives flow Mach numbers $M_{\perp}=0.5$ and $M_{\|}=0.17$.

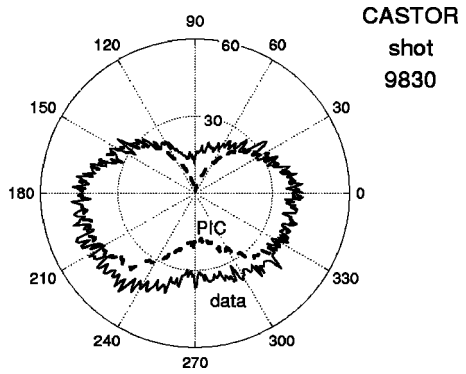

FIG. 10. Calculated GUNDY code polar diagram (dashed curve) corresponding to the fitted Mach numbers of the previous figure. The data are the thin full curve. In general, it is not possible to fit the entire angular range with the models. There seems to be excess ion current collected by the top and bottom of the probe.

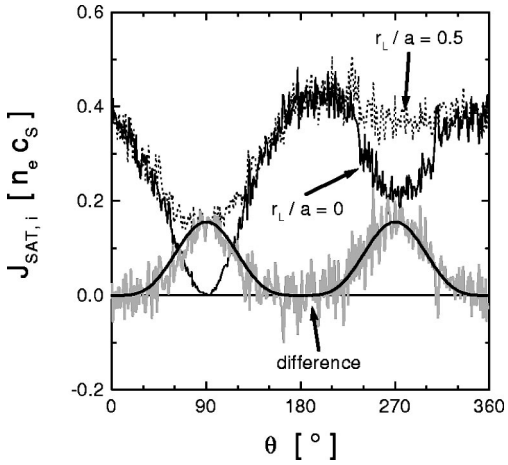

FIG. 11. A comparison of GUNDY ion current calculations with (dotted curve) and without (full curve) a finite Larmor radius. The difference is plotted in gray.

be fitted by the models. The excess current has been empirically parametrized, highlighting the need to include an additional cross-field transport term for grazing magnetic field angles.[15]

The model assumptions represent an asymptotic parameter regime that does not correspond to experimental reality. The models treat an infinite, uniform plasma with an infinitely high magnetic field and density such that the Larmor radius r_L and Debye length λ_D are infinitely smaller than the cross-field dimension a of the probe:

$$\frac{r_L}{a}, \frac{\lambda_D}{a} \rightarrow 0.$$

Work has begun to quantify the perpendicular ion transport to the top and bottom of the probe by improving the GUNDY code. The first step consists of allowing for finite Larmor radii. This is done by adding a sinusoidally varying perpendicular velocity to all ions. The amplitudes are chosen randomly to produce a Maxwellian distribution of Larmor radii. For now collisions are not included, so the ions' magnetic moments remain constant during the ion lifetime in the simulation region. The new GUNDY code was run with the fitted flow speed of Fig. 9. One run was done with ratio $r_L/a=0$ and a second with $r_L/a=0.5$. The current is increased on the top and bottom of the probe (Fig. 11), but is unchanged on the left and right sides. The magnitude of the additional current is identical on the top and bottom despite the large perpendicular drift speed. We do not yet know if this is a general result; simulations at other drift speeds are needed. In any case, it is apparent that the extra current could be due to finite Larmor radius effects. The magnitude of the effect, as well as the angular extent of it, will certainly depend directly on the degree of magnetization of the ions.[29]

V. SENSITIVITY TO MISALIGNMENT

To correctly separate the perpendicular from the parallel flow requires very accurate measurement of the angle between the rotating Mach probe and the magnetic field. We can anticipate the effect of misalignment analytically using the Van Goubergen model. The upstream-to-downstream current ratio as a function of magnetic field angle is given by

$$\frac{1}{c}\ln R = M_{\parallel} - M_{\perp}\cot\,\alpha,$$

where R is the current ratio, α is the true angle, and c is a constant given by the model

$$c = 2[1 + 0.14\,\cosh(M_{\parallel}/0.862)].$$

A linear fit of the logarithm against the cotangent gives directly the components of the flow vector. If there is a systematic error $\Delta\alpha$ of the angular reference, then the apparent characteristic becomes

$$\frac{1}{c}\ln R = M'_{\parallel} - M'_{\perp}\cot\alpha',$$

where the primes denote the falsely deduced values and $\alpha' = \alpha + \Delta\alpha$. One hopes that $\Delta\alpha$ is small compared to $\alpha \approx \pi/2$ so that

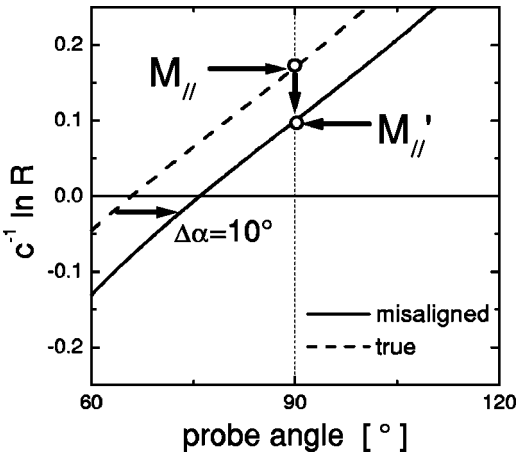

FIG. 12. The effect of an angular misalignment is to shift the experimental cotangent curve horizontally. The fitted parallel Mach number will change because it is obtained from the intersection of the curve with α=90°, whereas the perpendicular Mach number is unchanged because it is derived from the slope.

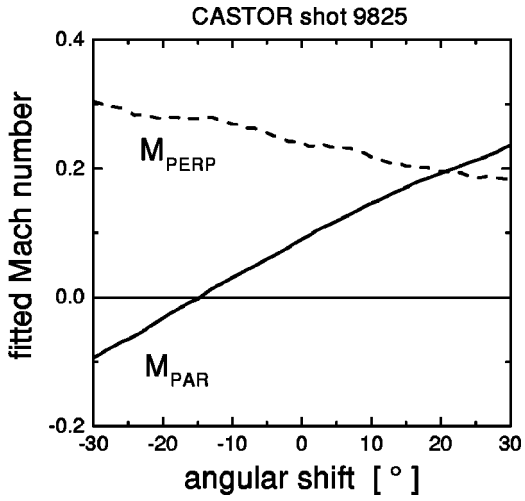

FIG. 13. Fitted Mach numbers obtained for different angular shifts of the polar diagram. The perpendicular Mach number is not much affected, but the parallel Mach number is.

$$\cot(\alpha+\Delta\alpha)\approx\cot\,\alpha-\tan\,\Delta\alpha,$$

yielding

$$\frac{1}{c}\ln\,R\approx M_{\parallel}'+M_{\perp}'\Delta\alpha-M_{\perp}'\cot\,\alpha'.$$

By equivalence with the correct expression, we find

$$M_{\perp}'\approx M_{\perp}$$

and

$$M_{\parallel}'\approx M_{\parallel}-M_{\perp}\Delta\theta.$$

The perpendicular speed is not sensitive to misalignment, whereas the parallel speed can be affected if the perpendicular speed is high enough. This is because an angular shift displaces the cotangent curve along the horizontal axis (see the illustration in Fig. 12). In Fig. 13 we show the result of varying the orientation of an experimental current distribution (CASTOR shot 9825) with respect to the magnetic field. The fitted perpendicular speed is not as sensitive to misalignment as is the parallel speed.

VI. CONCLUSIONS

Fluid and kinetic models give similar predictions for ion current collection by inclined, planar collectors (whether they be rotatable plates or surface elements of a round probe) in the angular range for which the model assumptions are valid. The Bohm–Chodura criterion plays a preponderant role in the fluid model, but supersonic, kinetic effects can occur under some conditions. To quantify the departure from purely guiding center collection to more complicated 2D collection mechanisms will require extensive kinetic simulations. For now, providing the magnetization is not too low ($r_L/a<0.5$), one can pragmatically eliminate magnetic field angles within $\pm30°$ of grazing incidence and suppose that the remaining polar diagram can be reliably fitted by the existing models. To firmly validate this experimental technique, a dedicated experiment is needed in which independent spectroscopic measurements of parallel and perpendicular flow are made simultaneously with probe measurements. Preferably, the experiment should be carried out in an apparatus with biasing capability so that the flows can be externally controlled. When building a multipin Gundestrup probe, we recommend minimizing the gap width between pin and housing, and measuring very accurately each pin angle. The precision of the flow measurement is limited by the uncertainty of the effective collecting area of the pins.

ACKNOWLEDGMENTS

We warmly thank František Jiránek (chief designer and contruction of mechanical parts) and Josef Zelenka (wires and circuits) of CASTOR for their excellent technical assistance. An insightful remark by Dr. Art Carlson inspired the discussion about the equivalence between the 1D and 2D models.

[1] J. Neuhauser, W. Schneider, R. Wunderlich, and K. Lackner, Nucl. Fusion **24**, 39 (1984).
[2] J. A. Boedo, G. D. Porter, M. J. Schaeffer *et al.*, *Proceedings of Contributed Papers*, 25th European Conference on Controlled Fusion and Plasma Physics, Prague, 1998, edited by P. Pavlo (European Physical Society, Petit-Lancy, 1998), Vol. 22C, p. 822.
[3] JET Team, Fusion Technol. **1**, 11 (1987).
[4] J. P. Coad, P. L. Andrew, J. D. Elder, S. K. Erents, H. Y. Guo, C. F. Maggi, G. F. Matthews, and P. C. Stangeby, *Proceedings of Contributed Papers*, 26th European Conference on Controlled Fusion and Plasma Physics, Maastricht, 1999, edited by B. Schweer, G. Van Oost, and E. Vietzke (European Physical Society, Petit-Lancy, 1999), Vol. 23J, p. 53.
[5] C. S. Pitcher, J. A. Goetz, B. LaBombard, B. Lipschultz, J. L. Weaver, and B. L. Welch, J. Nucl. Mater. **266–269**, 1009 (1999).
[6] M. Tendler and V. Rozhansky, Comments Plasma Phys. Control. Fusion **13**, 191 (1990).
[7] B. L. Stansfield, C. Boucher, J. P. Gunn, H. Guo, T. Fall, J. Mailloux, F. Meo, and B. Terreault, J. Nucl. Mater. **220–222**, 1121 (1995).
[8] C. S. MacLatchy, C. Boucher, D. A. Poirier, J. P. Gunn, B. L. Stansfield, and W. W. Zuzak, J. Nucl. Mater. **196–198**, 248 (1992).
[9] R. J. Armstrong and D. S. Darrow, Nucl. Fusion **34**, 1532 (1994).
[10] B. J. Peterson, J. N. Talmadge, D. T. Anderson, F. S. B. Anderson, and J. L. Shohet, Rev. Sci. Instrum. **65**, 2599 (1994).
[11] C. Xiao, K. K. Jain, W. Zhang, and A. Hirose, Phys. Plasmas **1**, 2291 (1994).
[12] V. Antoni, D. Desideri, E. Martines, G. Serianni, and L. Tramontin, Nucl. Fusion **36**, 1561 (1996).
[13] W. Y. Hong, E. Y. Wang, L. B. Ran, S. K. Yang, Y. D. Pan, L. Y. Chen, and S. J. Qian, J. Nucl. Mater. **241–243**, 1234 (1997).
[14] H. Van Goubergen, Ph.D. thesis, Universiteit Gent, 2000.
[15] K. Dyabilin, M. Hron, J. Stöckel, and F. Zacek, ''Rotating Mach probe for the measurement of the ion flows on CASTOR tokamak,'' *Proceedings of Contributed Papers*, 26th European Conference on Controlled Fusion and Plasma Physics, Budapest, 2000 (European Physical Society, Petit-Lancy, in press).
[16] J. Stöckel, G. Van Oost, J. P. Gunn, K. Dyabilin, and S. Nanobashvili, Bull. Am. Phys. Soc. **45**, 315 (2000).
[17] C. S. MacLatchy, C. Boucher, D. A. Poirier, and J. P. Gunn, Rev. Sci. Instrum. **63**, 3923 (1992).
[18] J. Stöckel, J. Badalac, I. Duran *et al.*, Plasma Phys. Controlled Fusion **41**, 577 (1999).
[19] J. P. Gunn, Czech. J. Phys. **48**, 293 (1998).
[20] H. Van Goubergen, R. R. Weynants, S. Jachmich, M. Van Schoor, G. Van Oost, and E. Desoppere, Plasma Phys. Controlled Fusion **41**, L17 (1999).
[21] I. H. Hutchinson, Phys. Fluids **30**, 3777 (1987).
[22] K.-S. Chung and I. H. Hutchinson, Phys. Rev. A **38**, 4721 (1988).
[23] P. C. Stangeby, Phys. Fluids **27**, 2699 (1984).
[24] S. I. Braginskii, in *Reviews of Plasma Physics*, edited by M. A. Leontovich (Consultants Bureau, New York, 1965), Vol. 1, p. 205.

[25]D. Poirier and C. Boucher, in Ref. 2, p. 1602.
[26]P. C. Stangeby, Phys. Plasmas **2**, 702 (1995).
[27]J. P. Gunn, C. Boucher, F. Meo, and B. L. Stansfield, Czech. J. Phys. **49/S3**, 219 (1999).
[28]M. Hron, I. Duran, J. Horacek, K. Jakubka, L. Kryska, J. Stöckel, F. Zacek, K. Dyabilin, S. Nanobashvili, I. Nanobashvili, M. Tendler, and G. Van Oost, Czech. J. Phys. **49/S3**, 181 (1999).
[29]J. P. Gunn, Phys. Plasmas **4**, 4435 (1997).